

# The Tank's Geometric Properties Effect on the Sloshing Wave Height and the Resulting Forces on the Roof

Ali Ebrahimi Hariri <sup>a\*</sup>, Yaghoub Mohammadi <sup>a</sup>

<sup>a</sup> Civil Engineering Department, University of Mohaghegh Ardabili, Iran

## ARTICLE INFO

### Keywords:

Geometric properties  
Sloshing height  
Upward force  
Sufficient non-zero freeboard

### Article history:

Received 6 April 2025  
Accepted 13 May 2025  
Available online 21 May 2022

## ABSTRACT

This paper outlines the effects of freeboard height sufficiency on sloshing wave characteristics, considering the geometric properties of rectangular tanks. Recorded ground accelerations of the 1999 Kocaeli and 1994 Northridge earthquakes are applied to the finite element model with different geometric assumptions. Both the frequency content of recorded ground motions and their PGA influence the sloshing wave responses. The geometric properties include the ratio of contained liquid height to tank length, wall elasticity, wall thickness, and freeboard height, considering tanks with and without the roof. The choice of roofed or roofless tanks significantly affects the sloshing properties because of non-zero insufficient freeboard influences. Sloshing height is studied for the roofless tanks, assuming sufficient freeboards. The upward force arising from inadequate freeboard shows the roofed tanks' sloshing wave characteristics, including various insufficient freeboards. For the roofless tanks, the rigidity assumption and the thickness reduction of elastic tanks reduce the sloshing height. The maximum sloshing height also decreases by decreasing the ratio of the contained liquid height to the tank length. So, the roofless tanks exhibit a clear trend in the tank geometric variations. The roofed tanks with zero insufficient freeboards also show a regular trend; however, the sloshing forces increase by decreasing the H to L ratio. But, tanks with insufficient non-zero freeboards do not indicate any steady trend for the geometric variation because of non-zero insufficient freeboard effects. A comparison of upward forces applied to the tanks' roof with their corresponding sloshing height time history shows the importance of zero or non-zero assumption for the freeboard height to control the sloshing characteristics. So, the sloshing wave responses are significantly dependent on the insufficient freeboard height assumption, although their responses depend on the tanks' various geometric properties.

## 1. Introduction

As crucial structures of modern society, liquid storage tanks must be designed to have no service limitations during earthquake excitation. Nevertheless, they are susceptible to high stresses under seismic excitation due to their considerable mass. The seismic-induced stresses may lead to cracking, leakage, or structural collapse. These structures' seismic responses are affected by earthquake properties and factors such as the fluid interaction, soil characteristics, flexibility of the body material, etc. [1, 2]. Among several parameters, earthquake-induced surface sloshing is one of the most important phenomena that has caused engineers and researchers to worry about it. Due to insufficient freeboard, the sloshing wave applies upward forces on the tanks' roof or spills liquid out for the roofless tanks. Considering this phenomenon's complexity, evaluation of the sloshing characteristics is of great importance [3-5].

Investigating the tanks' free surface sloshing characteristics, Edwards [6] applied the finite element method in combination with

\* Corresponding author.

E-mail addresses: [aliebrahimihariri@uma.ac.ir](mailto:aliebrahimihariri@uma.ac.ir) (A. Ebrahimi Hariri).



<https://doi.org/10.22080/ceas.2025.28937.1000>

ISSN: 3092-7749/© 2025 The Author(s). Published by University of Mazandaran.

This article is an open access article distributed under the terms and conditions of the Creative Commons Attribution (CC-BY) license (<https://creativecommons.org/licenses/by/4.0/deed.en>)

How to cite this article: Ebrahimi Hariri, A., Mohammadi, Y. The tank's geometric properties effect on the sloshing wave height and the resulting forces on the roof. Contributions of Civil Engineering and Applied Solutions. 2025;1(1): 36-52. doi:10.22080/ceas.2025.28937.1000.

the refined shell theory to study the sloshing, considering the induced stresses. Yang [7] investigated the tank structures' responses, assuming rigidity and elasticity for the empty state. Dogangun et al. [8] developed a three-dimensional finite element model of a rectangular tank, analyzing the tank by Lagrangian formulation. Ghaemmaghami [9] and Ghaemmaghami and Kianoush [10] examined the seismic behavior of two-dimensional tanks. They found that the walls' flexibility and the damping properties influence the structure's dynamic response behavior. Li and Wang [11] investigated the various methods of analyzing the sloshing in rectangular tanks. Parthasarathy [12] considered the effects of the natural frequencies of a rectangular and prismatic reservoir. They modeled sloshing by the volume fractionation (VOF) method and investigated the sloshing phenomenon by applying compressive load changes. Moslemi et al. [13] obtained the finite element response of free surface sloshing height by examining the parameters affecting rectangular tanks.

Milgram [14] performed a series of tests on partially filled tanks, studying the effect of abrupt changes of vertical velocity and free surface disturbances, and on the distribution of pressure on the roof. They also considered free surface disturbances. Minova et al. [15] and Minova [16] conducted a series of vibration plate tests on a rectangular tank to evaluate the roof's inserted pressure. They considered the natural frequencies effects. Chen et al. [17] calculated the dynamic compressive loads applied to the tank body due to the sloshing wave under a horizontal seismic excitation. They compared their numerical results with the experimental data. Kabiri et al. [5] investigated the sloshing wave impact force (SWIF) in tanks using numerical simulation based on the Boltzmann Network Method (LBM). They showed that the simple method recommended by the relevant codes and standards significantly measures the immersion force below the actual value. Lu et al. [18] calculated the impact force by a new method, including the sloshing height. Jena et al. [4] employed the meshless particle method to simulate the phenomena of intense free-surface sloshing flow. Base shear, overturning moment, forces applied against walls, and loads applied to the roofs were evaluated.

This study investigates the effects of tanks' geometric properties, especially non-zero insufficient freeboard, on the sloshing wave properties. Roofless tanks with sufficient freeboards and roofed tanks, considering bounded freeboards, are analyzed. The coupled problem of the liquid tank is analyzed employing the Lagrangian formulation. Different freeboards and boundary conditions are assumed. To do so, first, the effects of wall flexibility are studied considering walls with various thicknesses. In the following, rigid-roofed and roofless tanks with different geometric characteristics are supposed to investigate the freeboard height on the sloshing height and sloshing forces characteristics.

## 2. Conceptual review

Several methods have been proposed in computational fluid dynamics to model the fluid-structure coupling problem. These approaches are usually the Lagrangian, Eulerian, or a combination of both (ALE) approaches. In this study, the Lagrangian method formulates both the fluid and structure domains. On this account, the displacement as the variable describes both fluid and structural responses. So, the Lagrangian fluid is assumed to be linearly elastic, inviscid, and irrotational. The general two-dimensional stress-strain equation of a fluid element is [19].

$$\begin{Bmatrix} P \\ P_z \end{Bmatrix} = \begin{bmatrix} C_{11} & 0 \\ 0 & C_{22} \end{bmatrix} \begin{Bmatrix} \varepsilon_V \\ W_z \end{Bmatrix} \quad (1)$$

where  $P$  is the pressure,  $P_z$  is the rotational stress,  $C_{11}$  is the bulk modulus of fluid,  $C_{22}$  is the constraint parameter related to  $W_z$ ,  $\varepsilon_V$  is the volumetric strain, and  $W_z$  is the rotation about the axis  $Z$ .

Considering the pressure at the fluid free surface due to the sloshing effects, its stiffness matrix is calculated from the discretization of the following equation:

$$P = \gamma_w U_{fn} \quad (2)$$

where  $\gamma_w$  is the weight density of the fluid, and  $U_{fn}$  is the normal component of the free surface movement. In the following, the fluid total strain energy is employed to obtain the finite element approximation:

$$\Pi_e = \frac{1}{2} U_f^T K_f U_f \quad (3)$$

$$K_f = \sum k_f^e \quad (4)$$

$$k_f^e = \int_V B_f^{eT} C_f B_f^e dV^e \quad (5)$$

where  $U_f$  is the nodal movement vector,  $K_f$  is the stiffness matrix of the fluid system,  $K_f^e$  is the fluid element stiffness matrix,  $C_f$  is the elasticity matrix consisting of diagonal terms in Equation 1, and  $B_f^e$  is the strain-displacement matrix of the fluid element. In addition, the free surface motion intensifies the system's potential energy, which is considered as follows:

$$\Pi_s = \frac{1}{2} U_{sf}^T S_f U_{sf} \quad (6)$$

$$S_f = \sum s_f^e \quad (7)$$

$$S_f^e = \rho_f g \int_A h_s^T h_s dA^e \quad (8)$$

where  $U_{sf}$  and  $S_f$  are the vertical nodal displacement vector and the stiffness matrix of the free surface of the fluid system, respectively.  $S_f$  is the sum of the stiffness matrices of the free surface fluid elements,  $S_f^e$  is the stiffness matrix of the free surface fluid element,  $h_s$  is the vector consisting of interpolation functions of the free surface fluid element,  $\rho_f$  is the mass density of the fluid, and  $g$  is the acceleration due to gravity. Furthermore, the kinetic energy of the system can be written as:

$$T = \frac{1}{2} \dot{U}_f^T M_f \dot{U}_f \quad (9)$$

$$M_f = \sum M_f^e \quad (10)$$

$$M_f^e = \rho_f \int_V H^T H dV^e \quad (11)$$

where  $\dot{U}_f$  is the nodal velocity vector,  $M_f$  is the mass matrix of the fluid system,  $M_f^e$  is the sum of the mass matrix of the fluid elements, and  $H$  is the matrix consisting of interpolation functions of the fluid element.

Finally, the fluid finite element formulation of motion is calculated by the combination of Eq. 3, 6 and 9 as follows:

$$M_f \ddot{U}_f + K_f^* U_f = R_f \quad (12)$$

where  $\ddot{U}_f$ ,  $U_f$ ,  $K_f^*$  and  $R_f$  are the nodal acceleration, the nodal displacement, the system stiffness matrix including the free surface stiffness, and the time-varying nodal force vector for the fluid system, respectively.

The coupled equations of the fluid-structure system are obtained considering the boundary condition at the fluid-surface interface.

$$U_n^+ = U_n^- \quad (13)$$

where  $U_n^-$  and  $U_n^+$  is the normal portion of the interface structure and fluid displacement, respectively. By considering the interface condition and damping effects, the equations of motion of the coupled system to ground motions are written as [19]:

$$M_C \ddot{U}_C + C_C \dot{U}_C + K_C U_C = R_C \quad (14)$$

where  $M_C$ ,  $C_C$ , and  $K_C$  are the mass, damping, and stiffness of the coupled system.  $U_C$ ,  $\dot{U}_C$  and  $\ddot{U}_C$  are the vectors of the displacement, velocity, and acceleration, respectively.  $R_C$  is forces that are applied to the coupled system [19].

### 3. Finite element modeling of fluid-structure tank

#### 3.1. Geometric specifications

This study categorized the tank models into two groups in Table 1 shows their geometric properties. All tanks are short as H's ratio (height of the contained liquid) to L/2 (half of the tank length) varies from 1 to 1/3. The models are two-dimensional (see Fig. 1). Two different liquid heights of 5m and 10m are assumed. The thickness of all concrete tank walls ( $t_w$ ) is 0.5m. Additionally, the tank's (Hw) height is decided based on the height of the fluid (H) and the freeboard. The roofless tanks have sufficient freeboards. The roofed tanks have some bounded freeboards (1.00m, 0.75m, 0.50m, 0.25m, and 0.00m). The H5L15 tank walls are considered flexible in group 1 to investigate their thickness and flexibility effects on the sloshing phenomena. Accordingly, the H5L15 walls are initially rigid. In the following, their thickness is 0.3m, 0.4m, and 0.5m. The H5L15 flexible models are both roofed and roofless. The roofed tanks have a freeboard of 1m, but the roofless tanks' freeboard height is 2m.

**Table 1. Geometric properties of tank models.**

Group	Names	L (m)	H (m)	2H /L	Number of element
Group 1	H5L10	10	5	1	2482
	H5L15	15	5	2/3	3795
	H5L30	30	5	1/3	7718
Group 2	H10L20	20	10	1	9368
	H10L30	30	10	2/3	13948
	H10L60	60	10	1/3	27688

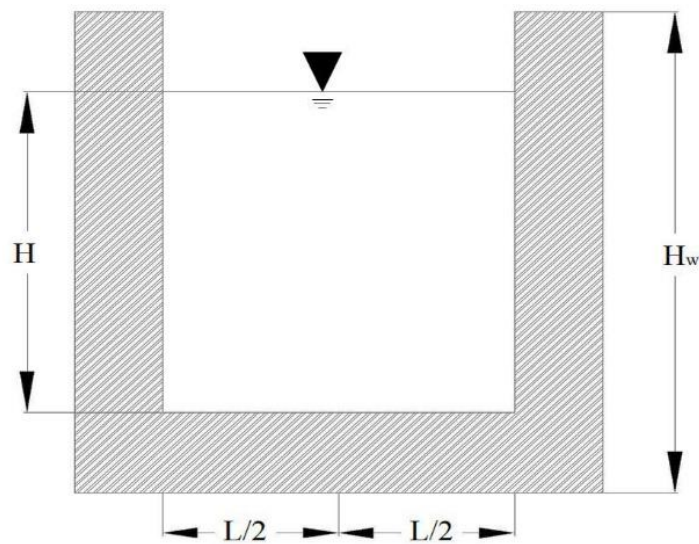


**Fig. 1. Tank model without a roof in a two-dimensional model.**

**3.2. Material properties and boundary conditions**

The 4-node shell elements model the tank's walls and the floor under plane strain assumption, considering 0.01m thickness for the tank along the Z-axis. The contact elements simulate the connection of the tank body to water, the tank body-roof, and the water-roof. The body and roof interfaces with the water are frictionless. But the internal friction angle between the body and the roof is 45 degrees. Table 2 shows the material properties for the walls, ceiling, and water. The equation of state of water, as the fluid of the container, is Mie-Gruneisen. Its material type is NULL.

**Table 2. material properties of water and concrete [13, 20].**

Water	Mass density (kg/m <sup>3</sup> )	Viscosity coefficient (Pa)	c (m/s)	$\gamma_0$	a	S <sub>1</sub>	S <sub>2</sub>	S <sub>3</sub>
		997	0.001	1480	0.5	0	2.56	1.986
Concrete	Mass density (kg/m <sup>3</sup> )	Young's modulus (Pa)	Poisson's ratio					
	2300	2.66E10	0.17					

The interaction between the structure and soil is neglected. All the bottom nodes of the floor slab in all directions are restrained. All tanks and liquid nodes are tied in the Z-direction, moving in the longitudinal direction X and vertical direction Y. Seismic excitations are only inserted in the X-direction. The time step  $\Delta t$  is 0.1 s.

**3.3. Seismic loads**

Two different recorded ground accelerations, including 1999 Kocaeli and 1994 Northridge, are applied. Figs. 2 and 3 show their time histories. In this study, PGA values for both records are scaled at 0.1g and 0.3g.

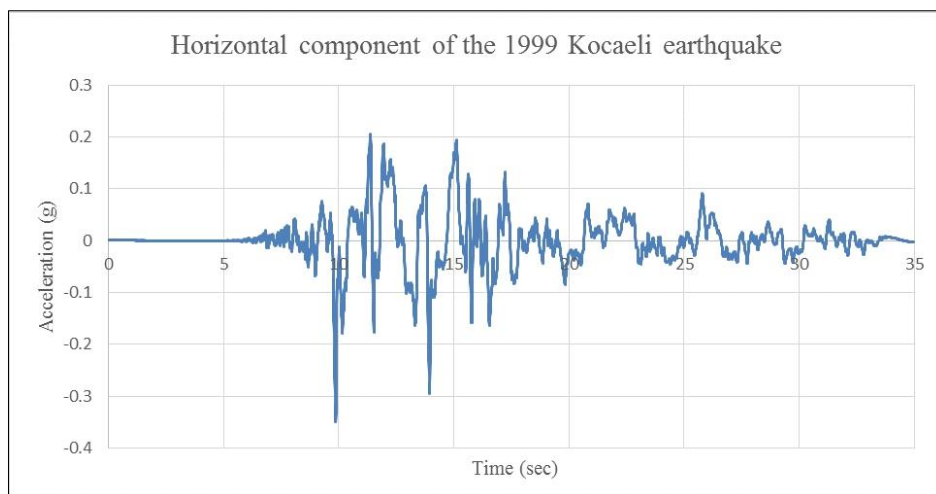


**Fig. 2. Horizontal component of the 1999 Kocaeli earthquake.**

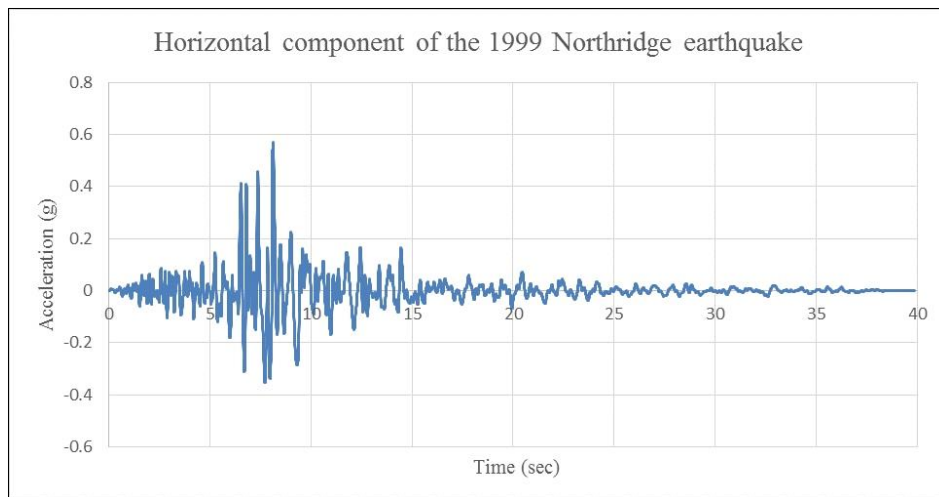


**Fig. 3. Horizontal component of the 1994 Northridge earthquake.**

Different studies include the earthquake frequency content as a factor that affects the sloshing phenomena. The response spectrum acceleration of earthquake ground motions is shown in Figs. 4 and 5 to investigate the frequency content. Besides, the ratio of peak ground acceleration (PGA) to peak ground velocity (PGV) is selected as a frequency content indicator [21]. Based on the classification proposed by Elnashai and Di Sarho [22], there are three categories which are: 1- low ratio when  $PGA/PGV < 0.8$ , 2- Intermediate ratio, including  $0.8 < PGA/PGV < 1.2$ , and 3- High ratio, including  $PGA/PGV > 1.2$ . For the Kocaeli earthquake, the  $PGA/PGV$  is less than 0.8, whereas for the Northridge earthquake, the ratio is about 0.8.

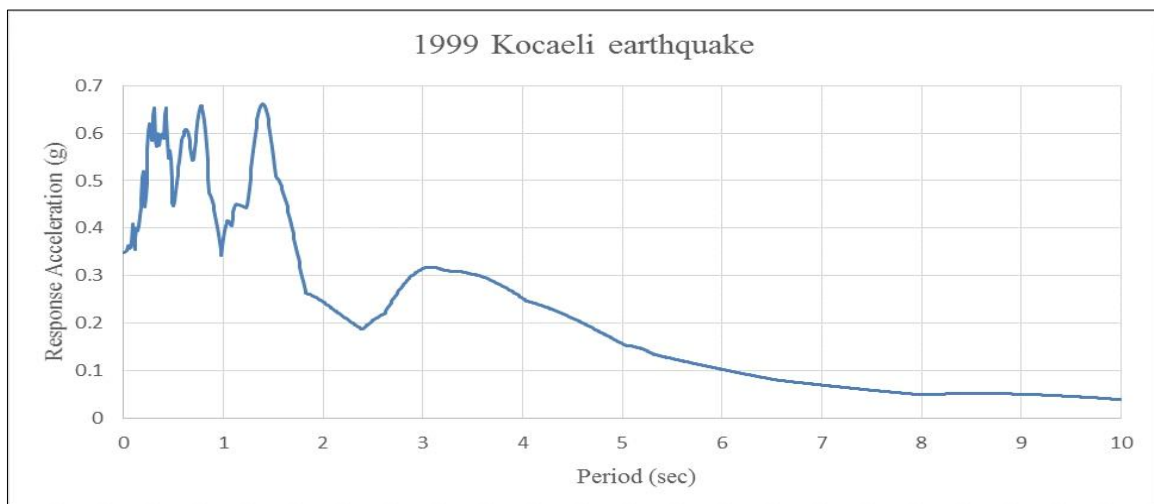


**Fig. 4. Response spectrum acceleration of the 1999 Kocaeli earthquake.**

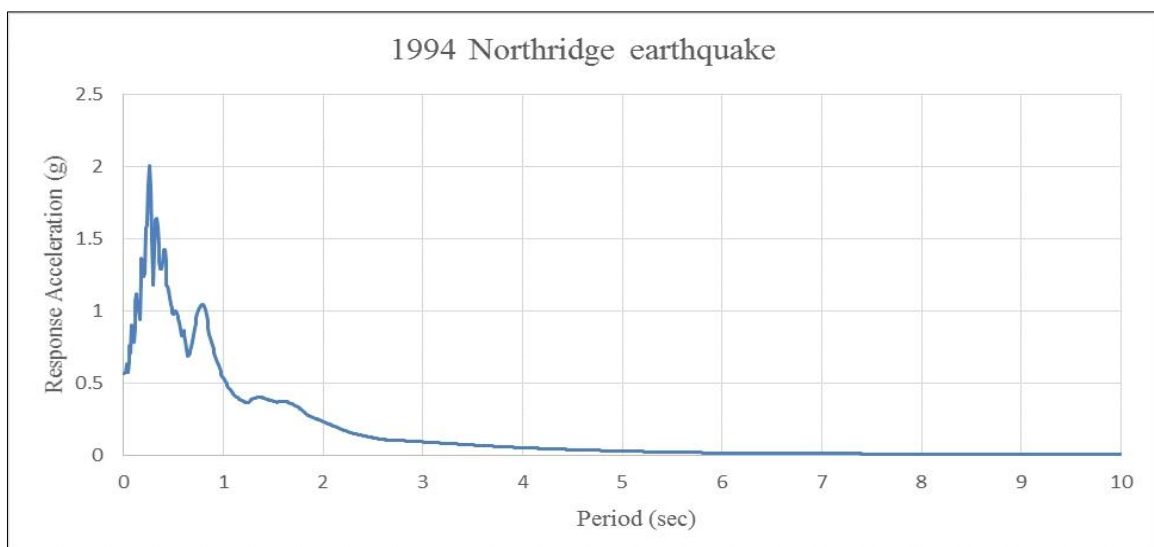


**Fig. 5. Response spectrum acceleration of the 1994 Northridge earthquake.**

### 3.4. Optimum size of the elements

Concerning the element size for reducing the computational cost, different element sizes are investigated, considering different mesh sizes varying from 0.01m to 0.6m. The length of the tank, water height, and freeboard are selected 15m, 5m, and 2m (H5L15 tank), respectively. The elastic wall thickness is assumed to be 0.5m. Fig 6 shows the artificial seismic excitation.

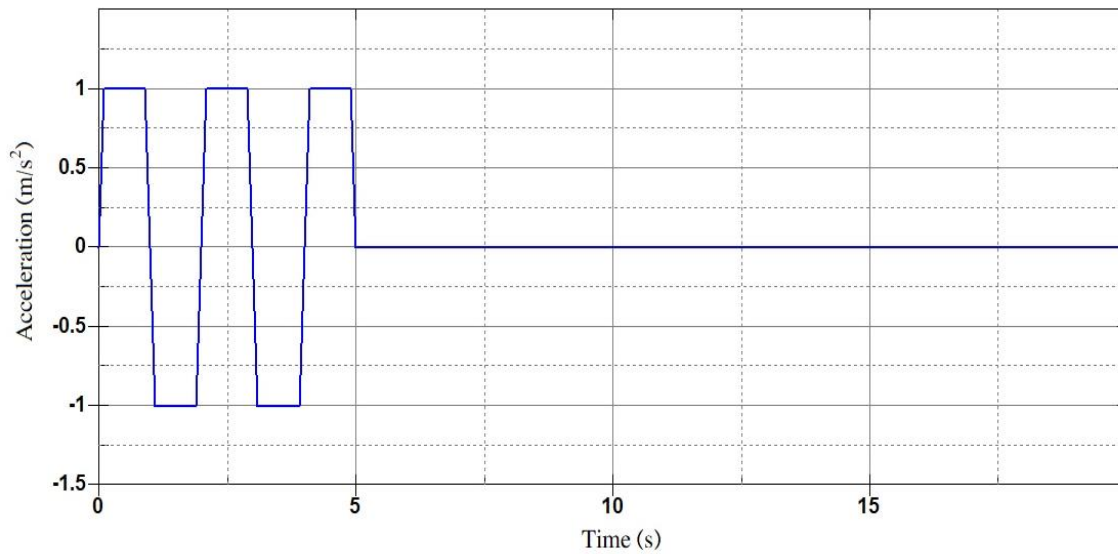


Fig. 6. artificial seismic excitation.

By applying artificial seismic excitation (Fig. 6), the maximum sloshing height is obtained. According to the results (Fig. 7), for the elements smaller than 0.2m, the sloshing height has no considerable change. So elements up to 0.2m are selected.

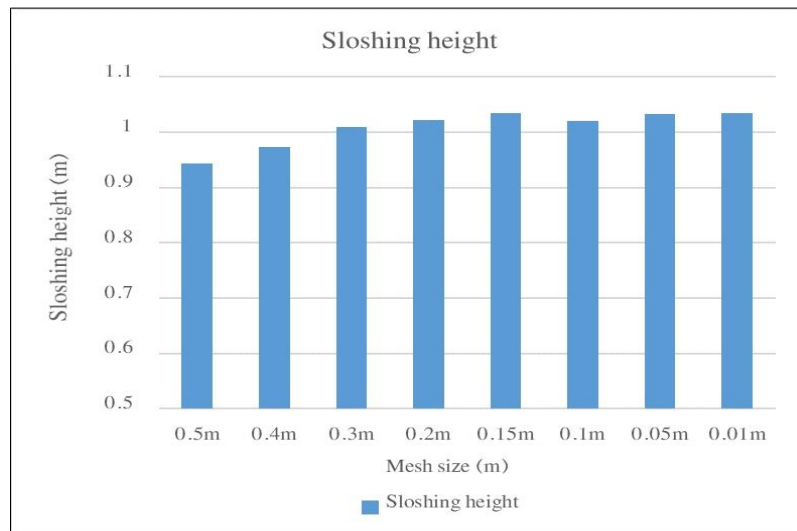


Fig. 7. Variation of sloshing height for different mesh sizes at both sides of the tank walls.

## 4. Results and discussion

### 4.1. Verification of finite element models and solution approach

The results presented by Vesenjak et al. [23] validate the finite element model developed in this study. Vesenjak et al. obtained the surface wave profiles created by stimulating a plexiglass water tank using Lagrangian, Eulerian, ALE, and SPH methods. The tank's length, width, and height were 1008mm, 196mm, and 300mm, respectively, while 60 percent of the tank (180mm) was full of water. The set was subjected to a horizontal acceleration of 30g for 80 milliseconds, and the point of 52 mm depth shows the time variation of water pressure.

The authors analyze the same model, including the Lagrangian method. Figs. 8 and 9 compare the results obtained by Vesenjak et al. [23] with those calculated by the authors. The time variation of water pressure fits the Vesenjak et al. responses precisely, as shown in Fig. 8. Fig. 9 presents the water-free surface under 30g seismic excitation at 30 ms for both models. The developed model is consistent with Vesenjak's results. So, the models established in this study lead to acceptable results.

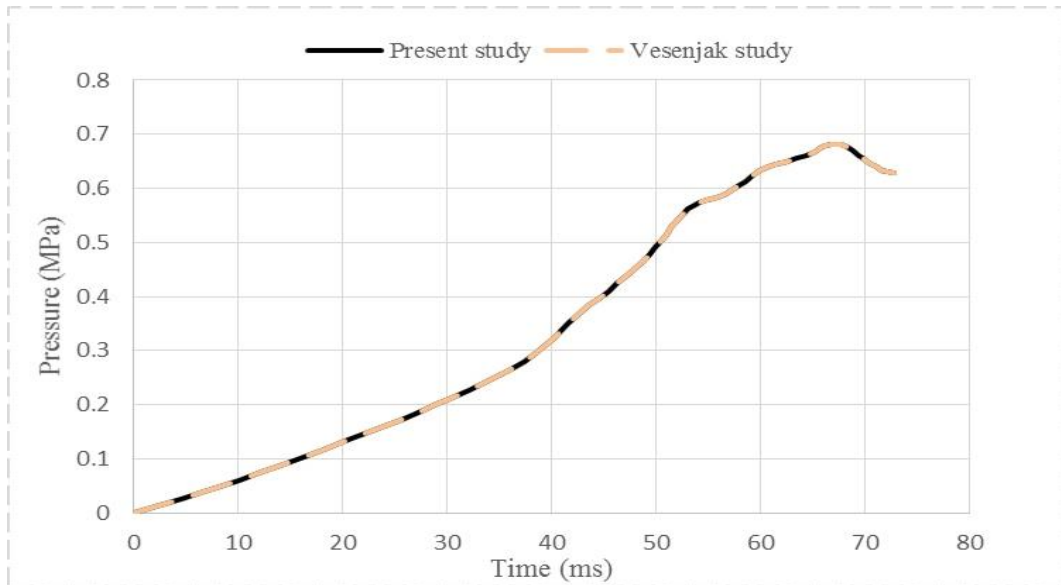


Fig. 8. The time variation of water pressure [22].

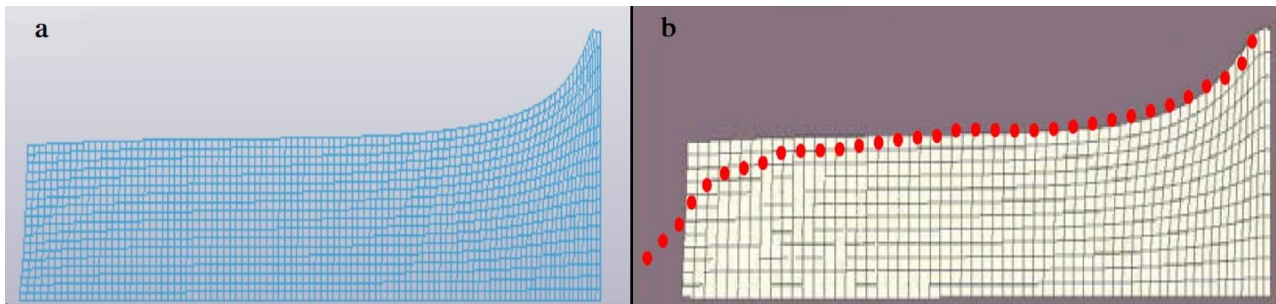


Fig. 9. Free surface of the water under 30 g seismic excitation at the time 30 ms; a) the result of made model in this study, and b) Vesenjak article result [22].

4.2. Effect of thickness and flexibility (elastic or rigid) of walls

At first, the wall elasticity and thickness on the sloshing height and forces are studied. The tanks with a length of 15m and a height of 5m are modeled (H5L15 of group 1 tank). For these tanks, the walls are initially rigid with a 0.5m thickness. Next, the thicknesses of the elastic walls are 0.5m, 0.4m, and 0.3m. The freeboard is 1m and 2m for the roofed and roofless tanks, respectively. The floor's self-weight and dynamic excitation are inserted into the finite element models.

Table 3 shows the sloshing wave height and forces inserted into the tanks' roofs and walls. These parameters decrease due to the wall rigidity under the same thickness assumption. Considering the elastic wall thickness variations, a reduction in thickness increases the sloshing height and the applied forces to the wall. But a different trend is observed for the forces applied to the roof. The load on the roof due to the sloshing wave impacts decreases by changing the wall thickness from 0.4 m to 0.3m. It seems that such distinctness shows the importance of freeboard height effects on the sloshing waves and their dynamic properties. More detailed analyses study the freeboard height effects in the following sections.

Table 3. Sloshing height and the resulting force on the roof and wall of tanks, considering different wall assumptions.

Result type	0.5 m wall thickness rigid	0.5 m wall thickness elastic	0.4 m wall thickness elastic	0.3 m wall thickness elastic
Sloshing height (m)	1.26	1.33	1.36	1.44
Force applied to the wall (kN)	73.3	118.8	120.4	122.7
Force applied to the roof (kN)	20.1	20.25	26.41	24.7

4.3. Rigid tanks

Although the walls' rigidity reduces the sloshing wave's effects, the previous section shows that results depend on the assumptions made for the freeboard height. This section investigates the influences of rigid tanks' geometric characteristics on the sloshing phenomenon, focusing on the freeboard sufficiency. The tanks are rigid to simplify the calculations and reduce the analysis time.

As mentioned, short tanks with 2H/L ratios of less than one are excited by two earthquake records. Fig. 10 shows two different tanks' schematic views, one without a roof and the other for the tank with a ceiling.

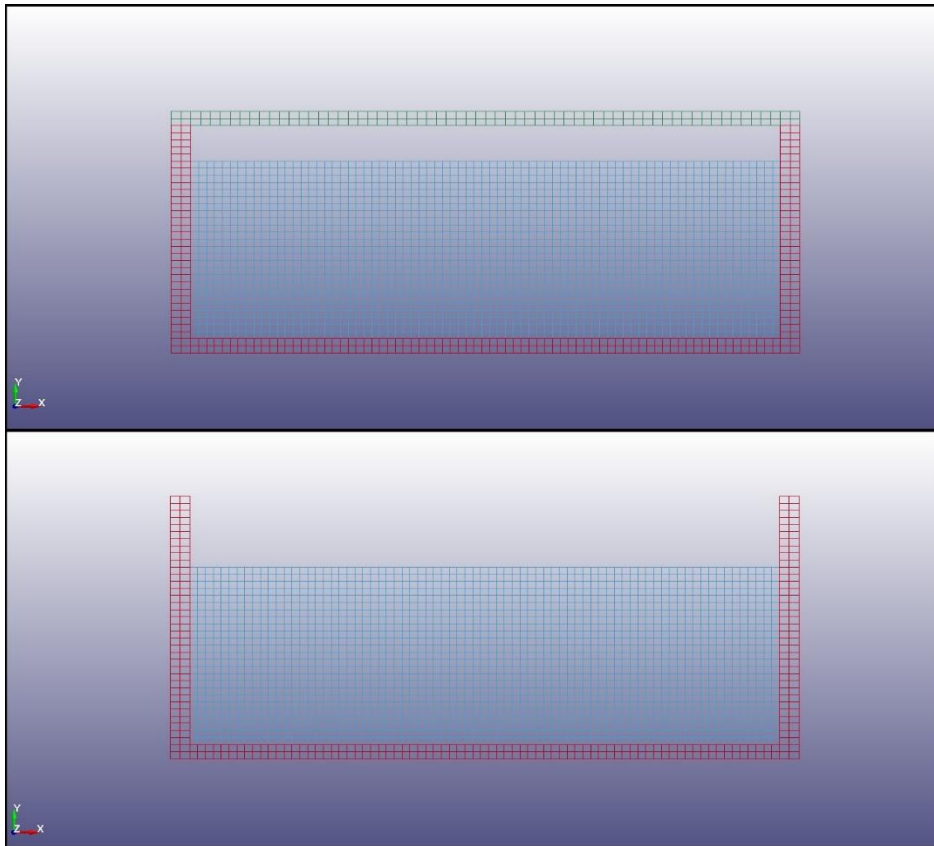


Fig. 10. Water sloshing in the H5L15 tank with and without a roof.

4.3.1. Sloshing height

This section considers roofless tanks. As mentioned previously, two different seismic excitations (1999 Kocaeli and 1994 Northridge) are applied to the models, while both records are scaled at two different values of 0.1g and 0.3g. Fig. 11 shows the maximum sloshing heights of tanks. According to Fig. 11, the maximum sloshing height decreases with increasing tank length for constant H. Furthermore, for fixed L, the maximum sloshing height increases with increasing tank height. So, decreasing the H to L ratio of the tank leads to reducing the maximum sloshing height. Both seismic excitations at two different scaled PGAs show this trend.

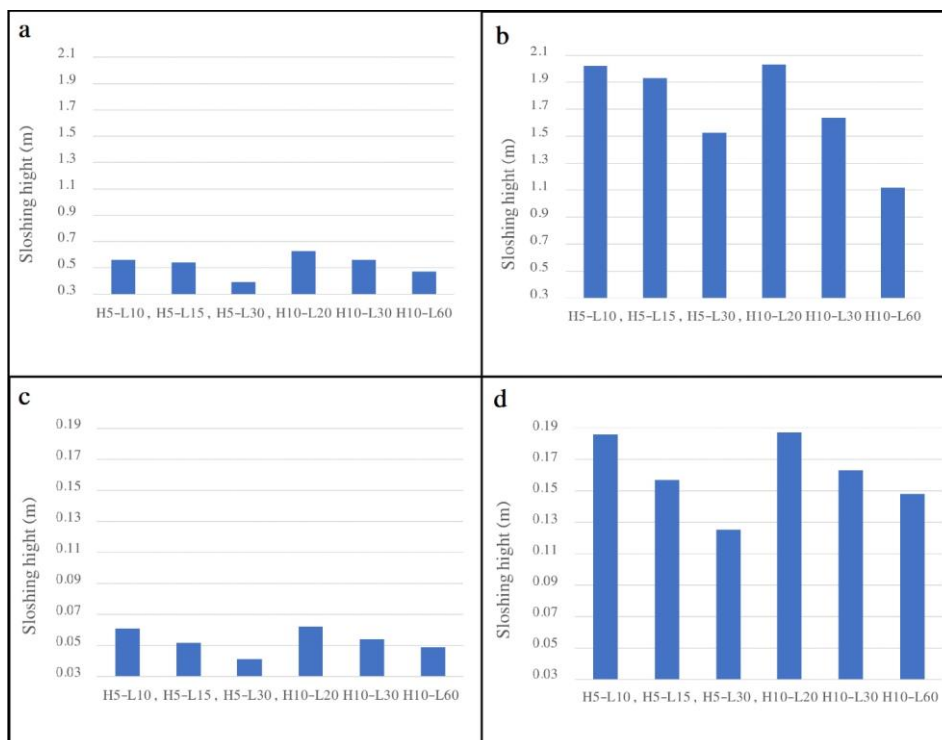


Fig. 11. Maximum sloshing height under a) Kocaeli 0.1g, b) Kocaeli 0.3g, c) Northridge 0.1g, and d) Northridge 0.3g scaled excitation.

Considering recorded ground accelerations, PGA, as expected, PGA's higher values (0.3g) induce higher sloshing height. For two different earthquake records, 1999 Kocaeli and 1994 Northridge, at the same scaled PGA, the Kocaeli earthquake record's sloshing height is much higher than the Northridge one. It seems the frequency content of the seismic excitation has significant effects on the sloshing phenomena. So, the PGA/PGV ratio is considered to investigate the frequency content of recorded ground motions. This ratio is less than 0.8 for the Kocaeli earthquake and is about 0.8 for the Northridge earthquake. So, the frequency content of these two ground motions is different.

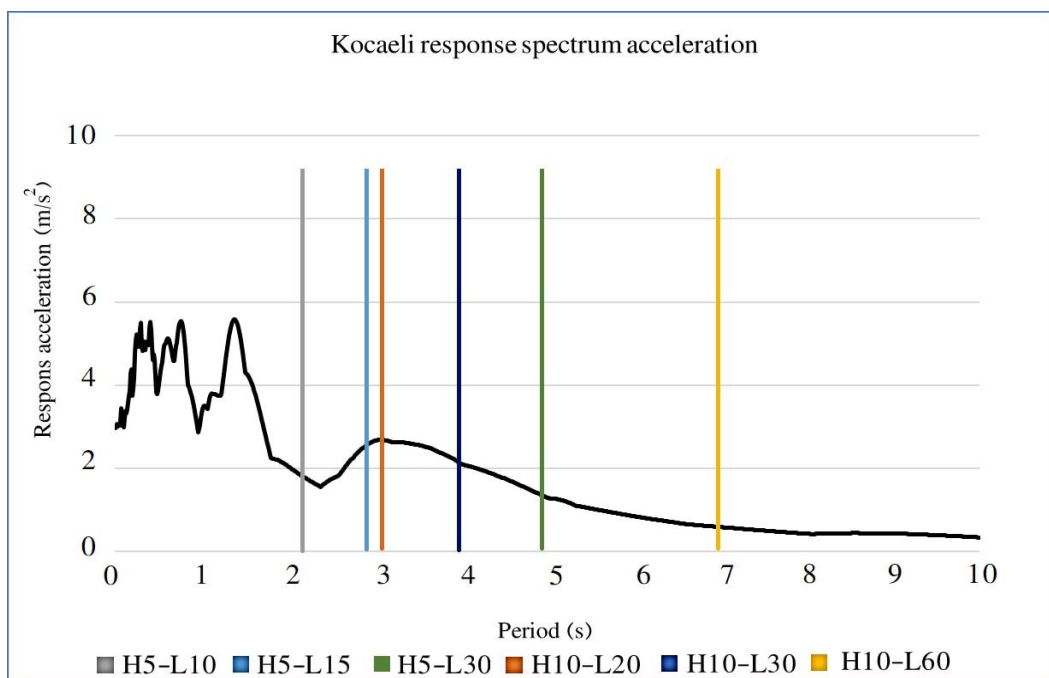
In the following, the natural period of the convective mode ( $T_c$ ) is calculated, investigating more detailed frequency content effects. It has been shown that the response of the convective mass controls the height of the sloshing wave. So, the natural period of the convective mode ( $T_c$ ) is calculated, investigating more detailed frequency content effects.  $T_c$  represents the geometry, length, and height of the convective part of the liquid.

Table 4 shows the system's fundamental period and the natural period of the first convective and impulsive mode from ACI 350 (see ACI350.3). Based on the results in Table 4, the vibrational period increased in constant H by the increment of L.

**Table 4. Modal analysis results.**

Tanks name	Group 1			Group 2		
	H5-L10	H5-L15	H5-L30	H10-L20	H10-L30	H10-L60
Fundamental period of the system (s) calculated by FEM	0.015	0.022	0.042	0.028	0.042	0.083
Natural period of the first convective mode of sloshing (s) calculated by ACI350	2.05	2.75	4.874	2.906	3.889	6.893
Natural period of the first impulsive mode (s) calculated by ACI350	0.148	0.1473	0.1474	0.5155	0.518	0.5199

Figs. 12 and 13 show the response spectrum acceleration of two recorded ground motions (scaled at 0.3g), whereas the fundamental period of different tanks is clarified. Based on figures 12 and 13, the Kocaeli earthquake component induces higher response spectrum acceleration over the first convective mode of sloshing. So, the sloshing height in Figure 13 is higher for the Kocaeli recorded ground motions at the same levels of PGA.



**Fig. 12. Natural period of the first convective mode of sloshing (s) calculated by ACI350 represented on response spectrum acceleration of 0.3g scaled Kocaeli earthquake.**

*4.3.2. Freeboard sufficiency and sloshing force*

This section investigates the freeboard sufficiency effects of roofed tanks, considering the same tank geometries as the previous section, except for freeboards, varying from 0m to 1m at increments of 0.25m, for each tank. The results show that the values of both maximum sloshing height and sloshing force peak occur on the sides of the tank wall. So, the design of the roofs at the sides of the tank requires more attention. Fig. 14 shows the maximum sloshing force under 0.1g scaled ground motion, whereas Fig. 15 presents the results of 0.3g scaled ground motion.

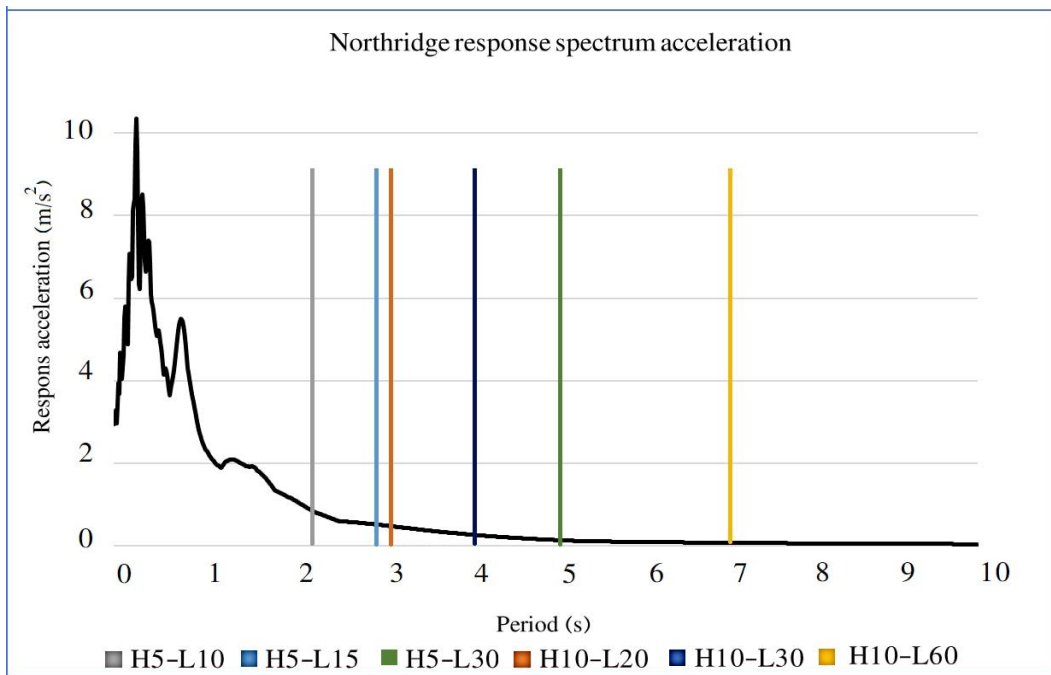


Fig. 13. Natural period of the first convective mode of sloshing (s) calculated by ACI350 represented on response spectrum acceleration of 0.3g scaled Northridge earthquake.

In both Fig. 14 and 15, there are some zero and non-zero responses. Zero force values indicate that the water inside the tank did not collide with the roof during the earthquake. A comparison of these zero sloshing forces with their corresponding sloshing height for the roofless tanks shows that the sloshing height calculated for the roofless tanks is less than the freeboard considered for the roofed tanks. So, zero sloshing forces present the sufficiency of the freeboard.

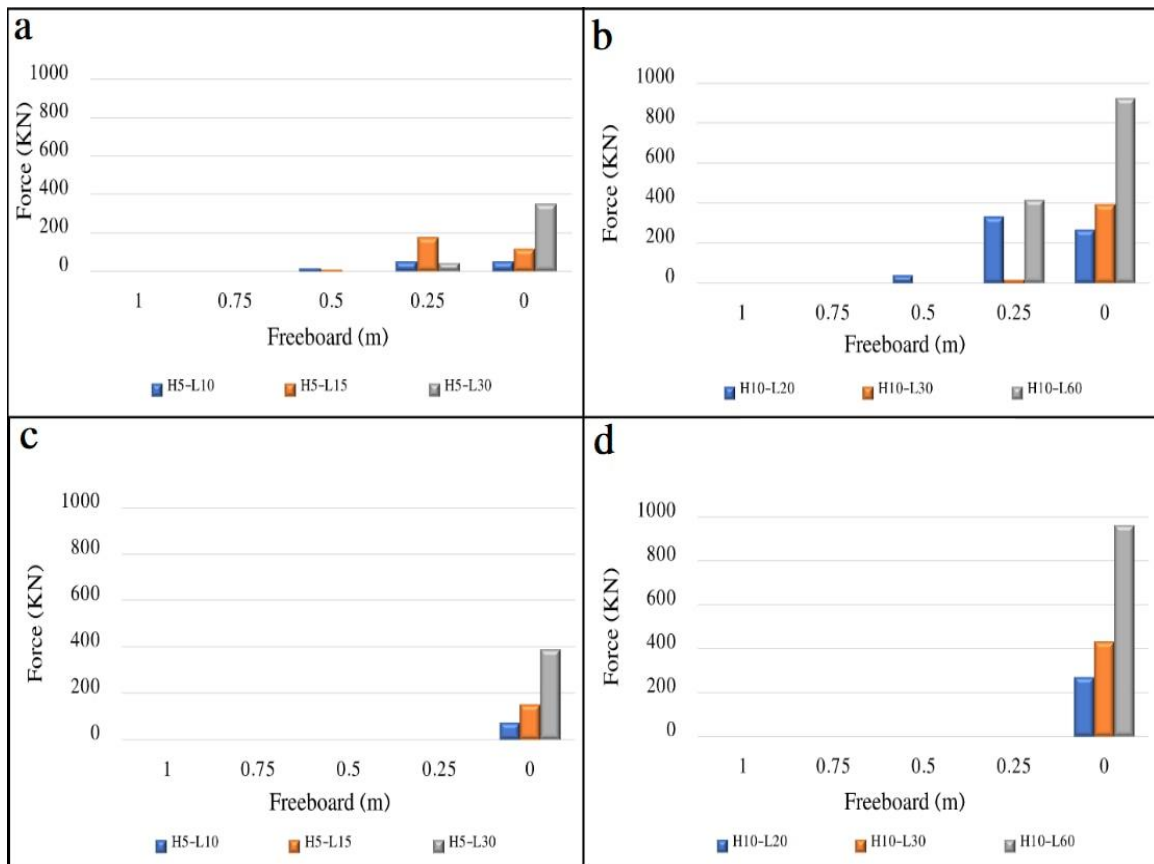
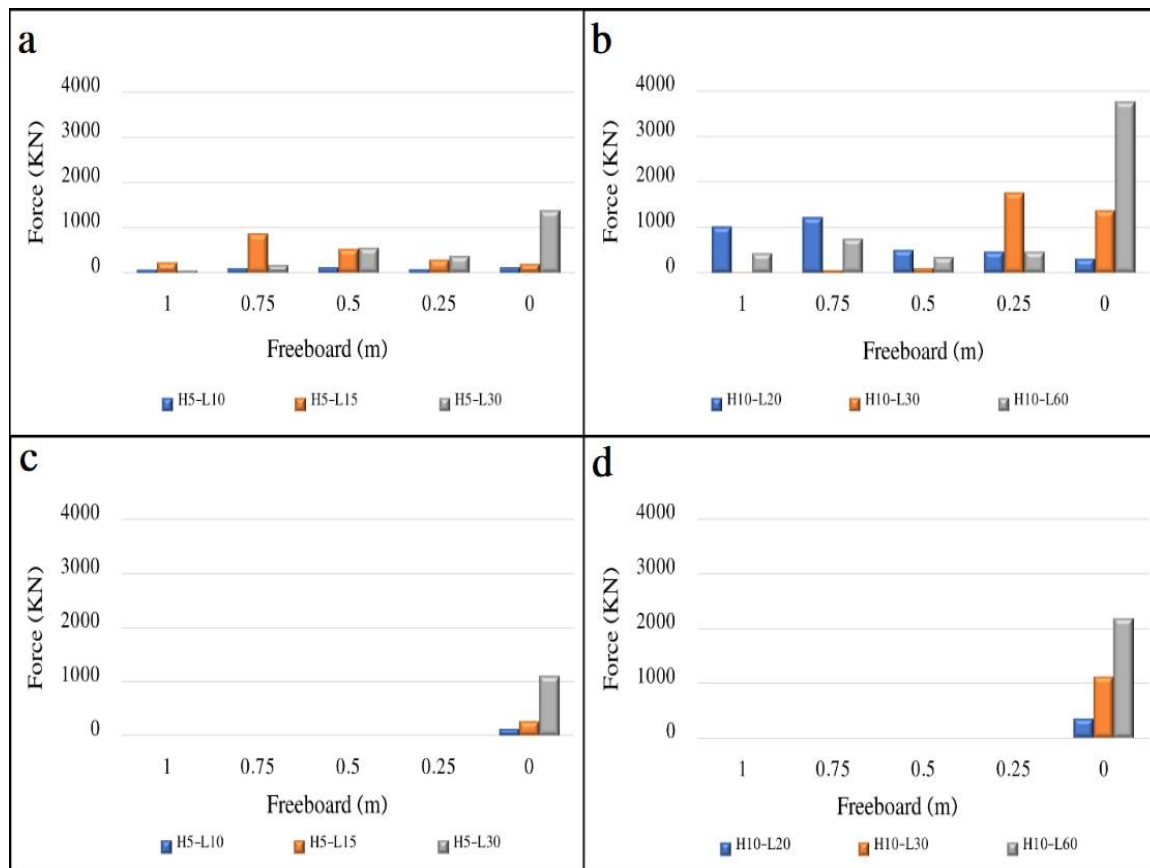


Fig. 14. Maximum sloshing forces under 0.1g scaled ground motions for different freeboard assumptions under a) Kocaeli excitation group1, b) Kocaeli excitation group2, c) Northridge excitation group1, and d) Northridge excitation group2.



**Fig. 15. Maximum sloshing forces under 0.3g scaled ground motions for different freeboard assumptions under a) Kocaeli excitation group1, b) Kocaeli excitation group2, c) Northridge excitation group1, and d) Northridge excitation group2.**

For the insufficient freeboard cases with zero freeboards, all tanks have similar response variations according to the H/L ratio. In these tanks, the sloshing forces increase by decreasing the H/L ratio. But, tanks with the non-zero freeboards do not show such a trend for the H/L ratio. Besides, the amount of force applied to the roof does not decrease as the freeboard increases. Accordingly, for the non-zero insufficient freeboards, responses do not show a constant trend considering different freeboard values.

In the case of insufficient freeboard, such differences between zero and non-zero freeboard responses on the sloshing force variations show the importance of an empty space on the sloshing wave's dynamic properties. It seems that the existence of air between the free surface and the roof influences the sloshing height and the upward forces inserted into the ceiling, allowing the free surface movement and its fluctuations. As a result, the effects of created sloshing waves on the system's frequency content and damping characteristics influence the responses.

Figs. 16 and 17 show the time history of the sloshing height at the right and left nodes located at the water's free surface for H10L30 and H5L15 tanks, respectively. The seismic load is 0.3g scaled Kocaeli earthquake. Three different freeboards are assumed in both figures: 1-sufficient freeboard, 2- 0.25m freeboard, 3- 0.5m freeboard.

As can be seen, the sloshing height and its oscillation process are highly dependent on the freeboard assumptions. Comparing sufficient freeboard by two non-zero sufficient ones (0.25m and 0.5m), changes in sloshing height variation trends are noticeable after reaching the sloshing height of the insufficient non-zero freeboard.

In both Figs. 16 and 17, sloshing height time histories for sufficient freeboard are symmetrical concerning the origin's axis. But, for 0.25m and 0.5m freeboards, the freeboard height controls the maximum sloshing height. When the sloshing waves collide with the roof, the other side of the water surface is at its peak value. For more detailed investigations, Figs. 18 and 19 illustrate the upward forces applied to the roof of H10L30 and H5L15 tanks for non-zero insufficient freeboard.

As can be seen (Figs. 18 and 19), the number of applied upward forces and their corresponding values are highly dependent on the freeboard height. This dependency may show the sloshing dynamic properties dependency on possible fluctuations in the free surface movement of water. This property is not available at the zero insufficient freeboard height. So, zero or non-zero assumptions for the freeboard height control the sloshing process, the values, and the number of forces. Table 5 shows the fundamental period of the roofed tanks with a 0.5m freeboard assumption. As presented in Table 5, the fundamental period increases by an increment of the tank length. Figures 20 and 21 show these period values in the response spectrum acceleration of 0.3g scaled Kocaeli and Northridge earthquakes, respectively.

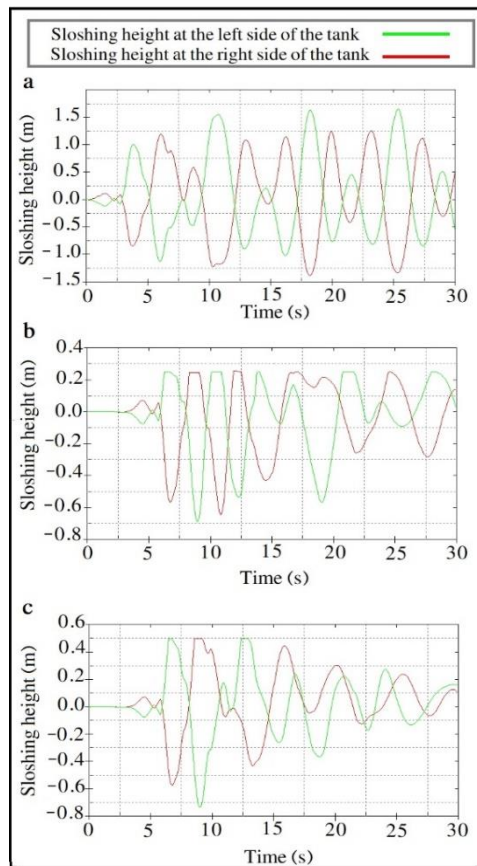


Fig. 16. Time history of sloshing height for H10L30 tank under 0.3g scaled Kocaeli earthquake: a) sufficient freeboard, b) 0.25m freeboard, and c) 0.5m freeboard.

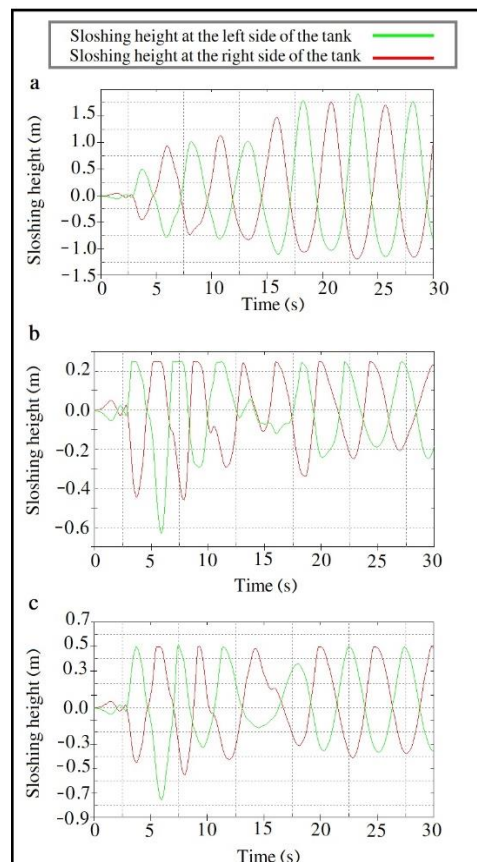


Fig. 17. Time history of sloshing height for H5L15 tank under 0.3g scaled Kocaeli earthquake: a) sufficient freeboard, b) 0.25m freeboard, and c) 0.5m freeboard.

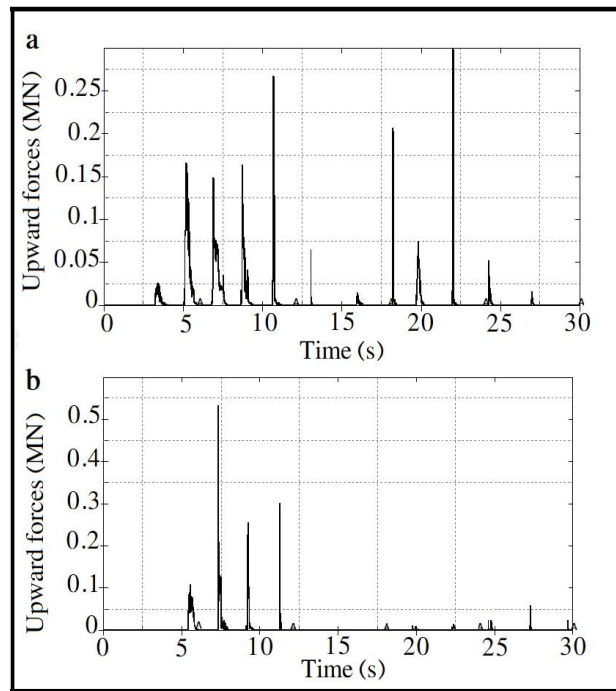


Fig. 18. Upward forces applied to the roof of H10L30 tank under 0.3g scaled Kocaeli earthquake: a) 0.25 m freeboard, and b) 0.5m freeboard.

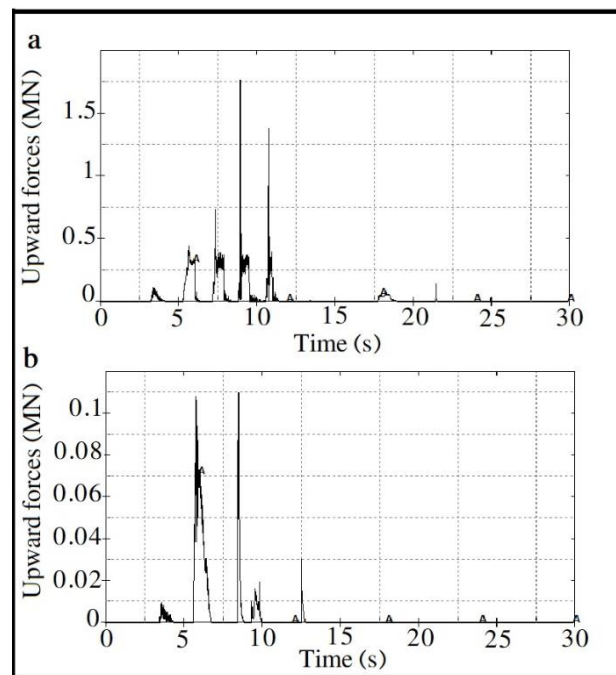


Fig. 19. Upward forces applied to the roof of H5L15 tank under 0.3g scaled Kocaeli earthquake: a) 0.25 m freeboard, and b) 0.5m freeboard.

Table 5. Modal analysis for the roofed tanks.

Tanks name	Group 1			Group 2		
	H5-L10	H5-L15	H5-L30	H10-L20	H10-L30	H10-L60
Fundamental period of the system (s) calculated by FEM	0.68	0.82	1.14	0.94	1.145	1.61

The upward forces caused by the Kocaeli earthquake record, in most cases, especially in zero freeboard cases, are higher than the Northridge earthquake record because of the lower PGA/PGV ratio value and frequency content. The models excited by the Kocaeli earthquake due to the lower frequency value will experience more stimulation of the convective part of the tank's water rather than the Northridge record. So, both the natural period ( $T_c$ ) of the tank's convective mode and the earthquake's frequency content affect the sloshing forces.

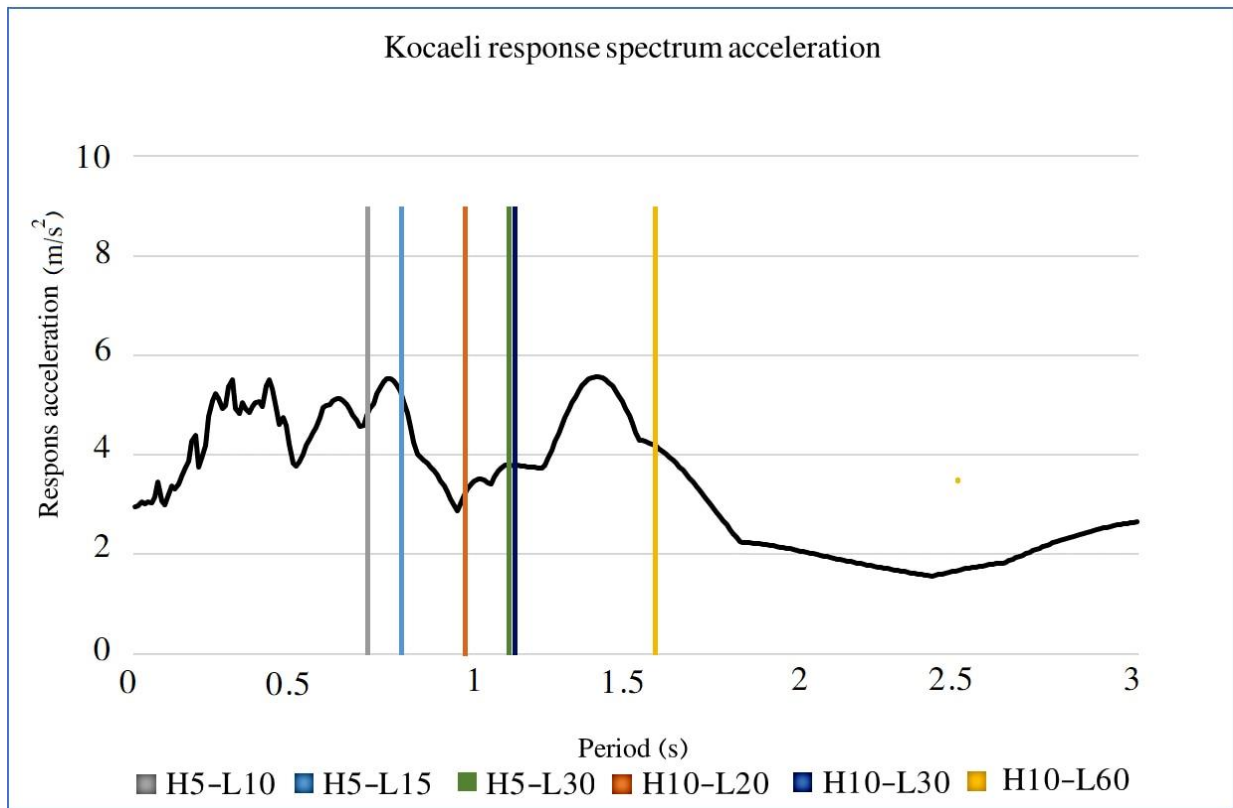


Fig. 20. Fundamental period of the (s) calculated by FEM represented on response spectrum acceleration of 0.3g scaled Kocaeli earthquake.

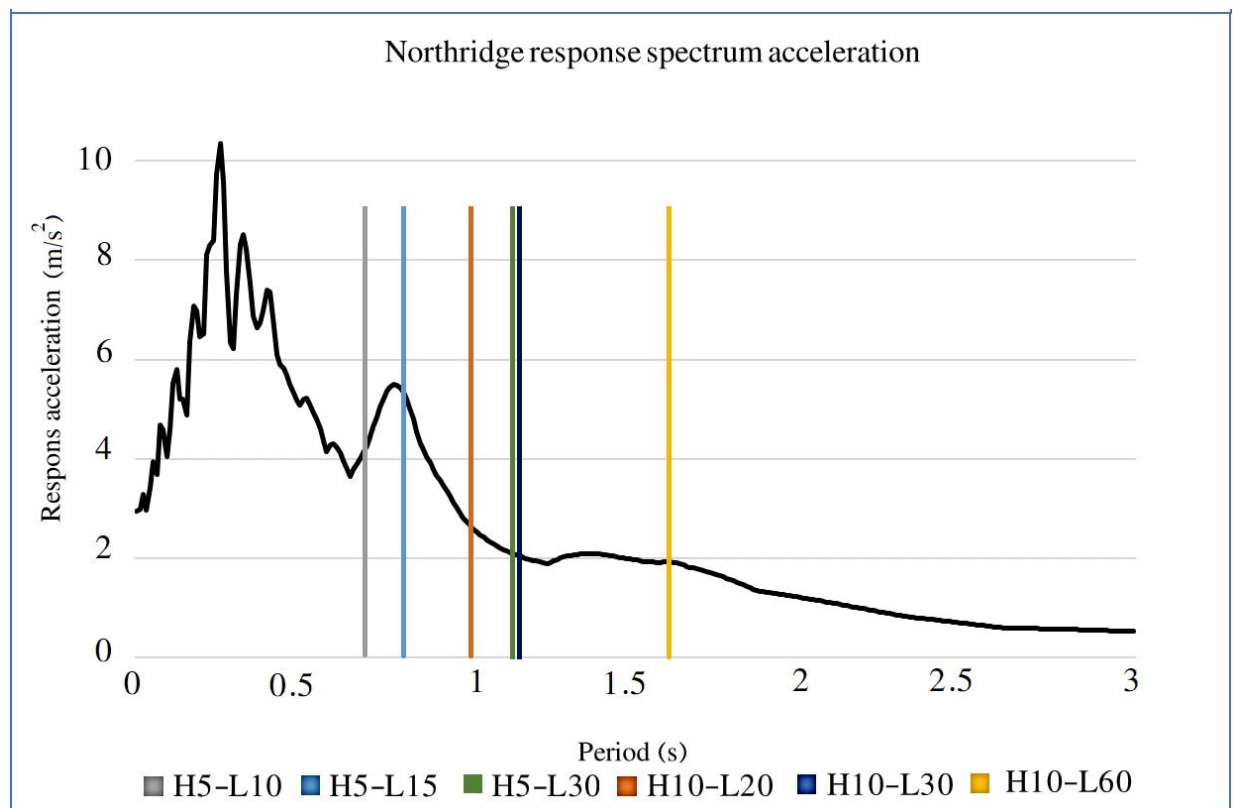


Fig. 21. Fundamental period of the roofed tank (s) calculated by FEM represented on response spectrum acceleration of 0.3g scaled Northridge earthquake.

Next, the effects of tank length on the upward load on the roof due to the sloshing wave's impacts are investigated. Figs. 22 to 24 show the sloshing height time history and upward forces of H5L10, H5L15, and H5L30. The freeboard is selected as 0.5m, and the seismic load is 0.3g scaled Kocaeli earthquake. The sloshing time history belongs to the roofless tank, while the upward forces correspond to the roofed ones. As can be seen, the number of upward forces from sloshing waves increases by reducing the tank length, although their values decrease.

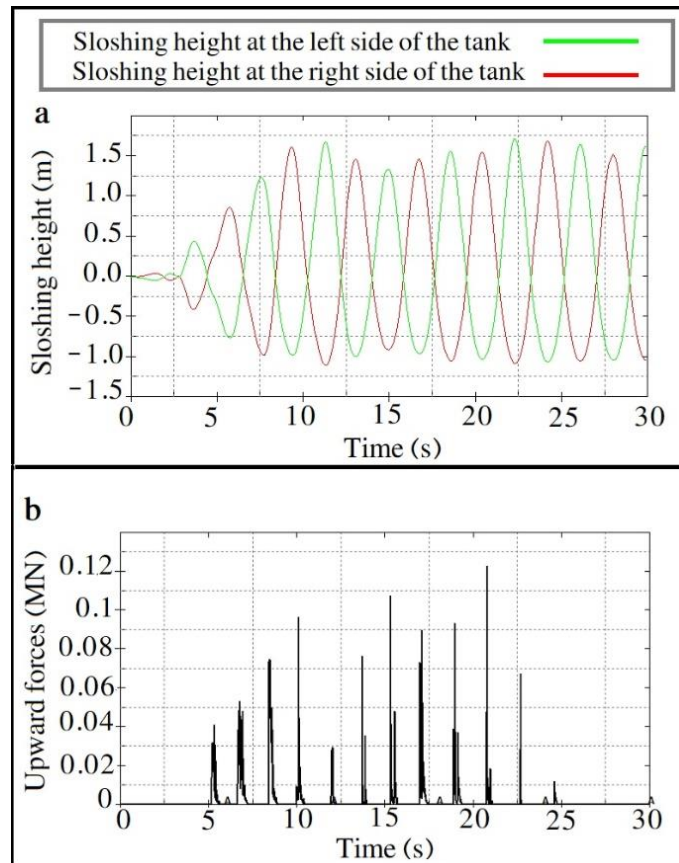


Fig. 22. H5L10 tank under 0.3g scaled Kocaeli earthquake-0.5m freeboard: a) sloshing time history, and b) upward forces

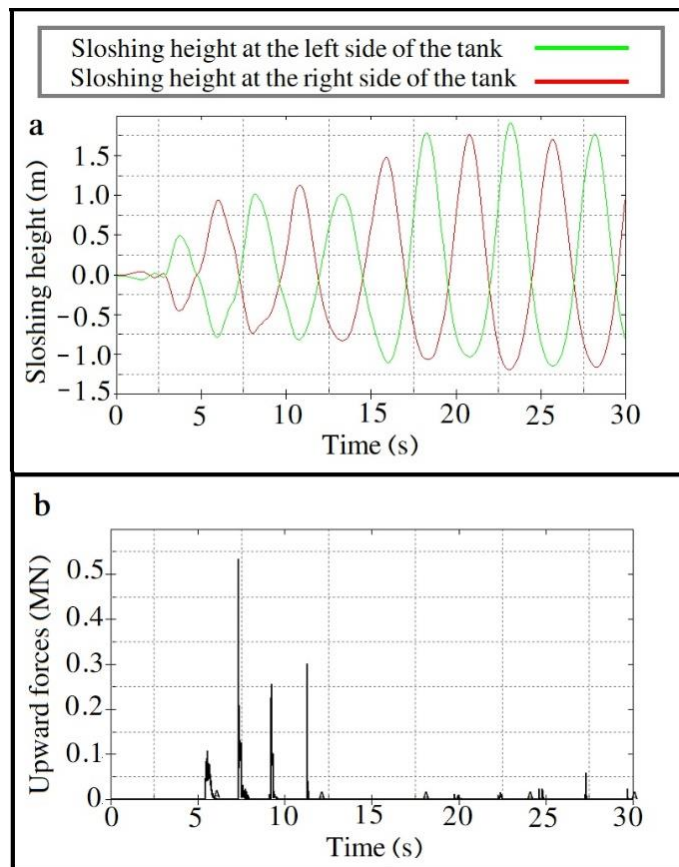


Fig. 23. H5L15 tank under 0.3g scaled Kocaeli earthquake-0.5m freeboard: a) sloshing time history, and b) upward forces

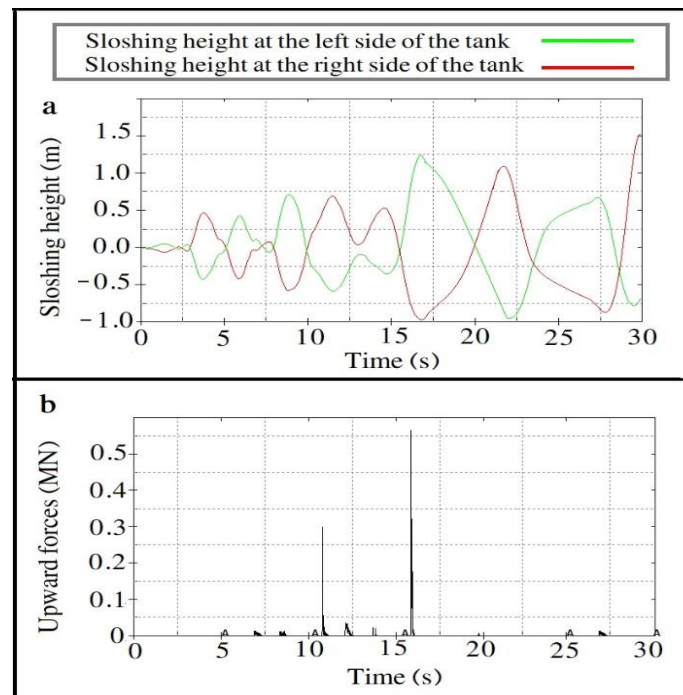


Fig. 24. H5L30 tank under 0.3g scaled Kocaeli earthquake-0.5m freeboard: a) sloshing time history, and b) upward forces

## 5. Conclusion

This study investigates the effects of the freeboard height sufficiency on sloshing waves' dynamic characteristics, including roofed and roofless tanks, considering different tank geometric properties. Seismic loads are the 1999 Kocaeli and 1994 Northridge earthquakes, in which their PGAs are scaled at 0.1g and 0.3 g. In all cases, both scaled ground motions of 0.3g produce higher sloshing height or upward forces. Additionally, the frequency content of earthquake records influences the responses. Based on the results, the tank wall rigidity reduces the sloshing height and forces arising from sloshing phenomena. For the elastic tanks, reduction of wall thickness reduces both the sloshing height and forces applied to the wall, but upward forces applied to the roof do not decrease regularly. Such irregular patterns show the effects of the freeboard height. For the rigid roofless tanks with sufficient freeboard, there is a clear trend of sloshing height variation due to the geometric change. In these tanks, the maximum sloshing height decreases by reducing the ratio of the height of the contained liquid to the tank length. Next, rigid-roofed tanks are studied considering different freeboards. There are two different responses for the roofed tanks: 1- the sloshing force is zero, which indicates the sufficiency of freeboard height. 2- Sloshing force is non-zero, which demonstrates insufficient freeboard height. In the case of insufficient freeboard, zero insufficient freeboard shows a clear trend for tank geometry variation. But non-zero insufficient freeboards have irregular responses. Such irregularity shows the importance of the empty space between the water-free surface and the tank's roof due to its effects on the system's frequency content and damping characteristics. So, zero or non-zero assumptions for the freeboard height mainly govern the sloshing process of roofed tanks.

## Statements & declarations

### Author contributions

**Ali Ebrahimi Hariri:** Investigation, Formal analysis, Resources, Writing - Original Draft.

**Yaghoub Mohammadi:** Conceptualization, Writing - Review & Editing.

### Funding

The authors received no financial support for the research, authorship, and/or publication of this article.

### Data availability

The data presented in this study will be available on interested request from the corresponding author.

### Declarations

The authors declare no conflict of interest.

## References

- [1] Mathew, A. K., Kumar Tomer, S., M, L. K., Student, P. G., Scholar, R. Effect of Soil-Structure Interaction in Seismic Analysis of Framed Structures Using Ansys. *International Journal of Engineering Development and Research*, 2015; 3 (3): 1–9.

- [2] Baghchesaraei, O. R., Lavasani, H. H., Baghchesaraei, A. Nonlinear Behavior of Circular Concrete Storage Tanks: History Pushover and Dynamic Loadings by Providing an Innovative Technique to Reduce the Seismic Response of Semi-Buried Tanks. *Applied Mechanics and Materials*, 2018; 878: 54–60. doi:10.4028/www.scientific.net/amm.878.54.
- [3] Aghajanzadeh, S. M., Mirzabozorg, H., Yazdani, H. SPH Technique to Study the Sloshing in Concrete Liquid Tanks. *Numerical Methods in Civil Engineering*, 2023; 8 (1): 1–17. doi:10.61186/nmce.2304.1015.
- [4] Jena, D., Biswal, K. C. Violent Sloshing and Wave Impact in a Seismically Excited Liquid-Filled Tank: Meshfree Particle Approach. *Journal of Engineering Mechanics*, 2018; 144 (3). doi:10.1061/(asce)em.1943-7889.0001364.
- [5] Kabiri, M. M., Nikoomanesh, M. R., Danesh, P. N., Goudarzi, M. A. Numerical and Experimental Evaluation of Sloshing Wave Force Caused by Dynamic Loads in Liquid Tanks. *Journal of Fluids Engineering, Transactions of the ASME*, 2019; 141 (11). doi:10.1115/1.4043855.
- [6] Edwards, N. W. A procedure for the dynamic analysis of thin walled cylindrical liquid storage tanks subjected to lateral ground motions [PhD thesis]. Ann Arbor (MI): University of Michigan; 1969.
- [7] Yang, J. Y. Dynamic behavior of fluid tank systems [PhD thesis]. Houston (TX): Rice University; 1976.
- [8] Doğangün, A., Durmuş, A., Ayvaz, Y. Static and Dynamic Analysis of Rectangular Tanks by Using the Lagrangian Fluid Finite Element. *Computers and Structures*, 1996; 59 (3): 547–552. doi:10.1016/0045-7949(95)00279-0.
- [9] Ghaemmaghani, A. Dynamic time-history response of concrete rectangular liquid storage tanks [Master's thesis]. Tehran (Iran): Sharif University; 2002. Persian.
- [10] Ghaemmaghani, A. R., Kianoush, M. R. Effect of Wall Flexibility on Dynamic Response of Concrete Rectangular Liquid Storage Tanks under Horizontal and Vertical Ground Motions. *Journal of Structural Engineering*, 2010; 136 (4): 441–451. doi:10.1061/(asce)st.1943-541x.0000123.
- [11] Li, Y., Wang, J. A Supplementary, Exact Solution of an Equivalent Mechanical Model for a Sloshing Fluid in a Rectangular Tank. *Journal of Fluids and Structures*, 2012; 31: 147–151. doi:10.1016/j.jfluidstructs.2012.02.012.
- [12] Parthasarathy, N., Kim, H., Choi, Y.-H., Lee, Y.-W. A Numerical Study on Sloshing Impact Loads in Prismatic Tanks under Forced Horizontal Motion. *Journal of the Korean Society of Marine Engineering*, 2017; 41 (2): 150–155. doi:10.5916/jkosme.2017.41.2.150.
- [13] Moslemi, M., Farzin, A., Kianoush, M. R. Nonlinear Sloshing Response of Liquid-Filled Rectangular Concrete Tanks under Seismic Excitation. *Engineering Structures*, 2019; 188: 564–577. doi:10.1016/j.engstruct.2019.03.037.
- [14] Milgram, J. H. The Motion of a Fluid in a Cylindrical Container with a Free Surface Following Vertical Impact. *Journal of Fluid Mechanics*, 1969; 37 (3): 435–448. doi:10.1017/S0022112069000644.
- [15] Minowa C, Ogawa N, Harada I, Ma DC. Sloshing roof impact tests of a rectangular tank. Argonne (IL): Argonne National Laboratory; 1994. Report No.: ANL/RE/CP-82360.
- [16] Minowa, C. Sloshing Impact of a Rectangular Water Tank (Water Tank Damage Caused by the Kobe Earthquake). *Nippon Kikai Gakkai Ronbunshu, C Hen/Transactions of the Japan Society of Mechanical Engineers, Part C*, 1997; 63 (612): 2643–2649. doi:10.1299/kikaic.63.2643.
- [17] Chen, Y. G., Djidjeli, K., Price, W. G. Numerical Simulation of Liquid Sloshing Phenomena in Partially Filled Containers. *Computers and Fluids*, 2009; 38 (4): 830–842. doi:10.1016/j.compfluid.2008.09.003.
- [18] Lu, D., Zeng, X., Dang, J., Liu, Y. A Calculation Method for the Sloshing Impact Pressure Imposed on the Roof of a Passive Water Storage Tank of AP1000. *Science and Technology of Nuclear Installations*, 2016; 2016. doi:10.1155/2016/1613989.
- [19] Mowafy, M., Salem, M., Salem, T., Anwar, A., Eldeeb, H. Seismic Performance of Concrete Gravity Dams. *The Egyptian International Journal of Engineering Sciences and Technology*, 2016; 16:1–10. doi:10.21608/eijest.2013.96783.
- [20] Kianoush, M. R., Ghaemmaghani, A. R. The Effect of Earthquake Frequency Content on the Seismic Behavior of Concrete Rectangular Liquid Tanks Using the Finite Element Method Incorporating Soil-Structure Interaction. *Engineering Structures*, 2011; 33 (7): 2186–2200. doi:10.1016/j.engstruct.2011.03.009.
- [21] Zhu, T. J., Tso, W. K., Heidebrecht, A. C. Effect of Peak Ground a/v Ratio on Structural Damage. *Journal of Structural Engineering*, 1988; 114 (5): 1019–1037. doi:10.1061/(asce)0733-9445(1988)114:5(1019).
- [22] Elnashai A, Di Sarno L. *Fundamentals of earthquake engineering: from source to fragility*. 2nd ed. Hoboken (NJ): John Wiley & Sons; 2015.
- [23] Vesenjok M, Mullerschön H, Hummel A, Ren Z. Simulation of fuel sloshing—comparative study. In: *Proceedings of the 3rd German LS-DYNA Forum; 2004 Oct 14–15; Bamberg, Germany*. p. 1–8.